

## Highly Ordered Mesoporous Carbon as Catalyst for Oxidative Dehydrogenation of Ethylbenzene to Styrene

Dang Sheng Su,<sup>\*,[a]</sup> Juan Jose Delgado,<sup>[a]</sup> Xi Liu,<sup>[a]</sup> Di Wang,<sup>[a]</sup> Robert Schlögl,<sup>[a]</sup> Lifeng Wang,<sup>[b]</sup> Zhe Zhang,<sup>[b]</sup> Zhichao Shan,<sup>[b]</sup> and Feng-Shou Xiao<sup>\*,[b]</sup>

**Abstract:** We demonstrate that mesoporous carbon without deposition of metal particles is a highly active catalyst. It exhibits both high activity and selectivity in oxidative dehydrogenation of ethylbenzene to styrene, as well as long catalytic stability when compared with activated carbon. Both the as-prepared mesoporous carbon and

the active coke formed during the initial stage of the reaction play an important role in the catalytic performance.

**Keywords:** dehydrogenation · ethylbenzene · heterogeneous catalysis · mesoporous materials · styrene

XPS and IR techniques reveal that the surface oxygen functional groups formed during the reaction are the active sites for the reaction. The ordered mesoporous structure is beneficial for mass transport in catalytic reaction exhibiting long term stability in contrast to activated carbon.

### Introduction

Synthesis of ordered mesoporous carbon materials with various structures has achieved great progress.<sup>[1]</sup> Such carbon materials are usually synthesized by carbonization of sucrose, furfuryl alcohol, resin, or other suitable carbon sources inside silica or aluminosilicate mesopores. The high surface areas and controllable pore sizes of the ordered mesoporous carbons with large pore volumes make it a promising candidate for many applications, such as for the storage of hydrogen and methane, as super capacitor, and for molecular separation.<sup>[2–11]</sup> In catalysis, ordered mesoporous carbons were used to support a high loading of platinum in a highly dispersed state. Even for a Pt loading of 50 wt %, a mean size of 2.5 nm of Pt particles could be maintained, leading to

a superior performance for O<sub>2</sub> reduction in a fuel-cell setup.<sup>[3]</sup> Recently, an ordered mesoporous carbon has been used for the assembly of a magnetically separable hydrogenation catalyst.<sup>[12]</sup> Magnetic nanoparticles are deposited on the external surface of mesoporous carbon protected by a thin carbon shell. Such magnetic carbon supports loaded with palladium as hydrogenation catalyst could be completely removed by a magnet from the reaction solution of the hydrogenation of octene. While in all the reported works (including those in electrocatalysis), ordered mesoporous carbons are only used as supporting materials, no effort has been made up to now to use mesoporous carbon itself as a catalyst.

In fact, mesoporous carbon with ordered and adjustable porosity, large pore size and pore volume, and high surface area<sup>[13]</sup> can be a candidate as a high performance catalyst in the gas-phase reaction. Carbon materials, especially nanostructure carbon, have been reported to be highly active catalysts for oxidative dehydrogenation (ODH) of ethylbenzene to styrene.<sup>[14,15]</sup> Herein, we report on the catalytic performance of highly ordered mesoporous carbon in the ODH of ethylbenzene to styrene synthesis. Searching for new catalysts for use in the synthesis of the styrene monomer has drawn a lot of attention as the monomers are needed in several polymer syntheses. The current industrial processes are based on metal-oxide catalysts working at high temperatures in excess of steam. Our results reveal that ordered mesoporous carbons are active and stable for the synthesis of styrene under more favorable reaction conditions (low temper-

[a] Dr. D. S. Su, Dr. J. J. Delgado, Dr. X. Liu, Dr. D. Wang, Prof. Dr. R. Schlögl  
Fritz Haber Institute of the Max Planck Society  
Faradayweg 4–6  
14195 Berlin (Germany)  
Fax: (+49) 30-8413-4401  
E-mail: dangsheng@fhi-berlin.mpg.de

[b] Dr. L. Wang, Z. Zhang, Z. Shan, Prof. F.-S. Xiao  
State Key Laboratory of Inorganic Synthesis  
and Preparative Chemistry & College of Chemistry  
Jilin University  
Changchun 130012 (China)  
Fax: (+86) 431-85168624  
E-mail: fsxiao@mail.jlu.edu.cn

ature, without steam, energy saving) than that of the industrial catalyst.

## Results and Discussions

Sucrose was used as a carbon source and SBA-15 as the template for the synthesis of CMK-3 mesoporous carbon.<sup>[1b]</sup>

Scanning electron microscopy (SEM) of the mesoporous carbon after the removal of the silica template reveals the highly ordered mesostructure replicated from SBA-15 (Figure 1A). Figure 1B shows the image obtained from transmission electron microscopy (TEM) of the mesoporous carbons. The images taken with the electron beams both paral-

lel with and perpendicular to the well-ordered arrays of channels confirm the well-ordered hexagonal mesostructure.

The catalytic performance of ODH of ethylbenzene to styrene over CMK-3 carbon at different temperature and flow rate are summarized in Table 1. The conversion of EB increases from 36% to 69% when the temperature is

Table 1. Comparison of styrene yields over CMK-3 carbon at different operation conditions.

Operation conditions	Conversion* [%]	Selectivity* [%]	Yield* [%]
350 °C, 10 mL min <sup>-1</sup> , O/EB = 5:1	36.1	77.7	28.0
375 °C, 10 mL min <sup>-1</sup> , O/EB = 5:1	51.2	77.8	39.8
400 °C, 10 mL min <sup>-1</sup> , O/EB = 5:1	69.0	76.0	52.4
350 °C, 5 mL min <sup>-1</sup> , O/EB = 5:1	74.1	62.0	45.9

[\*]Values obtained after 5 hour at the steady state.

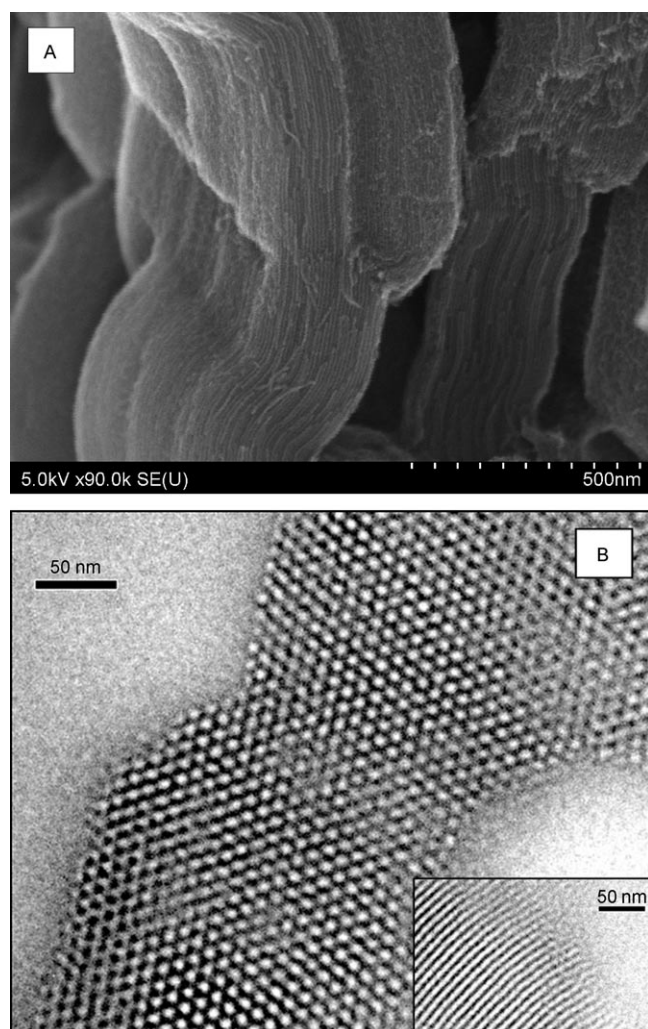


Figure 1. A) SEM image of CMK-3 carbons, B) TEM micrographs of CMK-3 carbon taken with the electron beam parallel the channels. The inset shows the channel structure.

changed from 350 °C to 400 °C, while the selectivity of EB to ST remains nearly constant (about 76%). The only by-products observed during the whole catalytic test were CO<sub>2</sub> and H<sub>2</sub>O, formed from the total oxidation of ethylbenzene. A change of flow rate from 10 mL min<sup>-1</sup> down to 5 mL min<sup>-1</sup> at 350 °C leads to an increased conversion of ethylbenzene (from 36% to 74%), but a decreased selectivity to styrene (from 77% to 62%). It is remarkable that an increase of the conversion rate by increasing the temperature did not change the selectivity of the catalyst, while the selectivity decreases by decreasing the flow rate. It seems that the high surface area of the CMK-3 would lead to the re-adsorption of the styrene even for short retention times, rendering a further reaction with oxygen and therefore, a total oxidation. For comparison, the yield of styrene at steady state over various tested nanocarbons is summarized in Table 2. CMK-3 carbon exhibits the highest selectivity under the given conditions. This material exhibits a styrene yield that is 2–4 times higher than the commercial carbon nanotubes.

Figure 2 displays the long term stability test of the ODH of ethylbenzene to styrene as a function of time on flow rate. After a short induction time at 400 °C and at a flow rate of 10 mL min<sup>-1</sup>, a selectivity of 76% EB to ST is achieved at a conversion of 69%. The high activity at the beginning of the reaction is accompanied by a slightly lower selectivity, but both level-off after 3 h. The C-balance of the inlet and outlet stream indicates that coking took place during the initial deactivation period at the beginning of the reaction, leading to a slightly lower concentration of carbon in the stream. After this period, the highly ordered CMK-3 carbon is structurally stable during the catalytic test.

The SEM image in Figure 3A reveals coke formation on the surface of the mesoporous carbon, and the TEM image in Figure 3B reveals that the mesopores are, to a certain degree, blocked by the coke formed at the beginning of the reaction. It is obvious that the mesoporous carbon is initially highly active for the ODH of EB, but coke formed at the beginning of the reaction may also be an active phase as has been reported by Cadus et al. for Al<sub>2</sub>O<sub>3</sub>.<sup>[22b]</sup> The combination of both the initial CMK-3 carbon and the active coke gives the high reaction rate shown in Table 1 and the long

Table 2. Comparison of styrene yields over various catalysts.

Sample	Operation conditions	Conversion [%]	Selectivity [%]	Yield [%]
CMK-3	400 °C, 10 mL min <sup>-1</sup> , O/EB = 5:1	69.0	76.0	52.4
Applied Science <sup>[a]</sup>	400 °C, 10 mL min <sup>-1</sup> , O/EB = 5:1	20.1	70.0	14.1
FC: CNF-PL <sup>[b]</sup>	400 °C, 10 mL min <sup>-1</sup> , O/EB = 5:1	26.2	64.9	17.0
FC: CNF-SC <sup>[c]</sup>	400 °C, 10 mL min <sup>-1</sup> , O/EB = 5:1	45.6	50.4	23.0

[a] Multiwalled carbon nanotubes (provided by Applied Science Ltd.). [b] Carbon nanofibers with platelet structure (provided by Future Carbon GmbH). [c] Carbon nanofibers with screw structure (provided by Future Carbon GmbH).

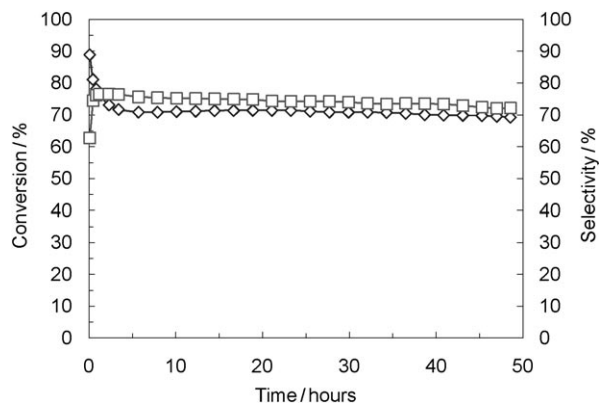


Figure 2. Conversion ( $\diamond$ ) and selectivity ( $\square$ ) of oxidative dehydrogenation of ethyl benzene to styrene over highly ordered CMK-3 carbon at 400 °C

term high stability shown in Figure 2. The electron-energy loss spectra (EELS) of the carbon K edge of the CMK-3 carbon before and after reaction are shown in Figure 4. The spectrum of the as-prepared sample exhibits a maximum at 286 eV, typical for the transition of carbon 1s electrons to the unoccupied  $\pi^*$  states. A broad feature from 292 eV to about 313 eV is attributed to  $1s\text{-}\sigma^*$  transitions. The as-prepared sample shows a sharper peak at the onset of the  $\sigma^*$  band than that of the sample after reaction. The prominent  $\pi^*$  and  $\sigma^*$  features in the as-prepared sample indicate a more graphitic feature of the prepared CMK-3 carbon. The EELS spectrum of the sample after reaction is quite similar to that of disordered carbon, revealing that the coke formed during the reactions differs in structure from the CMK-3 carbon.

The change in the pore structure of the mesoporous carbon is also confirmed by the nitrogen-isotherm plot shown in Figure 5. Nitrogen isotherms of CMK-3 before and after reaction exhibit typical IV curves, suggesting that both samples have mesopores with cylindrical shape. However, the sample after reaction shows a less obvious step at low partial pressures (before 0.4). After reaction, the BET surface area of the CMK-3 carbon is reduced from 983 m<sup>2</sup> g<sup>-1</sup> for the fresh catalyst to 211 m<sup>2</sup> g<sup>-1</sup>, which is obviously a result of the formation of coke during the reaction. However, the high stability shown in Figure 2 indicates that the loss of the surface area at the very beginning of the reaction does not have a strong influence to the catalytic performance of the CMK-3 carbon.

Figure 6A shows the C 1s X-ray photoelectron spectrum (XPS) of CMK-3 before and after reaction. The carbon spectra can be fitted to five peaks:<sup>[19,20]</sup> one peak for carbon atoms with bonds to carbon and/or hydrogen atoms

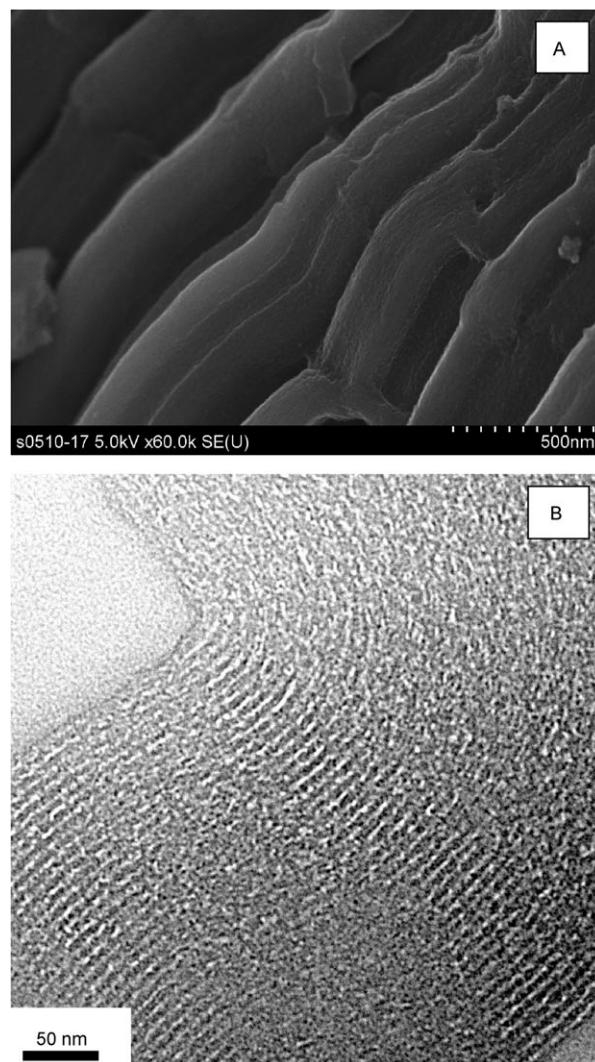


Figure 3. SEM (A) and TEM (B) micrographs of the CMK-3 carbon after 100 h catalytic test.

(C<sub>1</sub>, BE = 284.5 eV); three peaks for carbon atoms with one, two, and three bonds to oxygen atoms (C<sub>2</sub>, C<sub>3</sub>, C<sub>4</sub>; C–OH, C=O, COOH, BE = 285.0, 286.5, and 288.3 eV, respectively) and a  $\pi\text{-}\pi^*$  peak (C<sub>5</sub>, BE = 290). The C<sub>1</sub> peak had an asymmetrical shape, whereas the other peaks were symmetrical. C1s spectra before and after reaction were dominated by the intense asymmetrical C<sub>1</sub> and a smaller  $\pi\text{-}\pi^*$  (C<sub>5</sub>) peak, indicating a polyaromatic surface such as carbon black and carbon fiber.<sup>[19,21]</sup> The ODH reaction had a pronounced

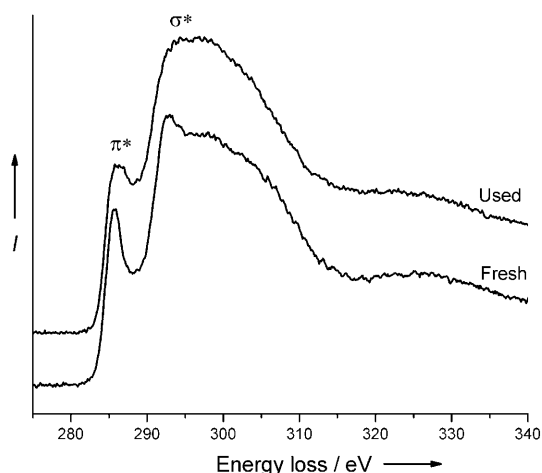


Figure 4. EELS spectra of carbon of the tested catalyst before (A) and after (B) reaction.

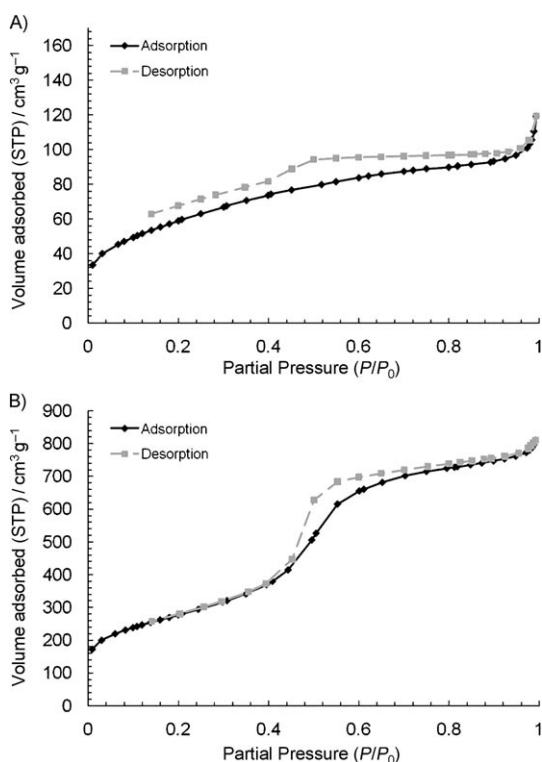


Figure 5.  $N_2$ -isotherms of CMK-3 carbon before (A) and after (B) reaction.

effect on the carbon spectra. After the reaction, the contribution of the  $C_1$  to the total C 1s spectrum decreases from 43 to 33%. The  $C_1$  peak becomes also broader, which can be related with the disordered structure of the coke. In fact, it was previously reported that styrene exhibit a peak at 284.9 eV.<sup>[23]</sup> It can be seen that the area of the  $C_3$  (C=O) peak increased after reaction, indicating an increasing carbonyl and quinone character of the surface. It is noticeable that the contribution of the  $C_4$  component in the C 1s spectrum increases after reaction.

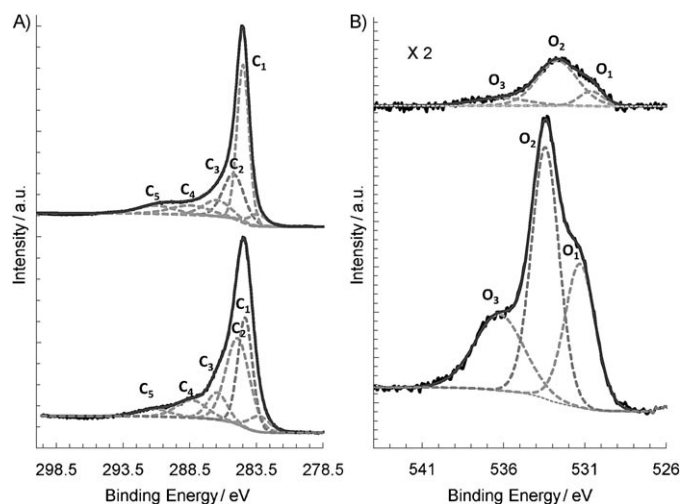


Figure 6. A) C1s and B) O1s XPS spectra of CMK-3 carbon before and after 100 h catalytic test.

Figure 6B shows the O 1s XPS of mesoporous carbon before and after reaction. The oxygen signal increases dramatically after reaction. The oxygen content on the surface of the fresh samples was around 1.5% and it increased to 17.8% after the catalytic test. The spectra were fitted using the model proposed by Xie and Sherwood<sup>[21]</sup> to three peaks corresponding to chinoidic carbonyl groups ( $O_1$ , BE = 531.2–531.6 eV), C–OH and/or C–O–C groups ( $O_2$ , BE = 533–534 eV), and chemisorbed oxygen and adsorbed water ( $O_3$ , BE = 535.4–536 eV).<sup>[21]</sup> These results are in good concordance with the C 1s spectra. The presence of strongly basic sites has been reported as active sites during the ODH reaction.<sup>[15,22]</sup> The obtained results correspond to the fact that carbonyl-quinone groups are the active sites in the ODH reaction.<sup>[22]</sup>

The IR spectra of the CMK-3 before and after reaction are displayed in Figure 7. The  $1713\text{ cm}^{-1}$  band is associated with the C=O vibrations of carboxyl, lactone, or ketone groups. The peaks observed in the range from  $1559$  to  $1509\text{ cm}^{-1}$  can be assigned to carbon skeleton vibration of the aromatic ring. The strong peaks at  $1222\text{ cm}^{-1}$  were attributed to the combination of C–O stretching vibration. The peaks at  $1041\text{ cm}^{-1}$  may be associated with C–O or C–

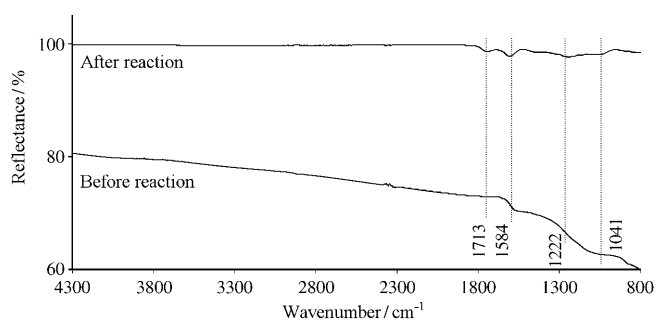


Figure 7. Attenuated total reflectance IR spectra of CMK-3 carbon before and after 100 h catalytic test.

O–C vibrations of ester, ether, phenol, or carboxyl groups. Clearly, after 100 h of the catalytic test, the sample exhibits an obvious peak at  $1713\text{ cm}^{-1}$ , which is a typical signal of surface C=O groups. This result confirms that surface C=O groups are catalytically active for ODH. These groups would be formed by the activation of molecular oxygen on the basal planes of the graphite layers or on the defected carbon surface. The possible presence of acetophenone-type carbon in coke may also cause the vibration at  $1713\text{ cm}^{-1}$ .

Nanocarbons with graphitic structure, such as carbon nanofilaments, onion-like carbons,<sup>[14]</sup> and carbon nanotubes,<sup>[15]</sup> are reported to be highly active for the ODH of ethylbenzene to styrene. The common characteristic of the mentioned nanocarbons are the long-range ordering of the graphitic  $sp^2$  structure. The activity of nanocarbon in ODH of ethylbenzene to styrene is assigned to the surface defects of the nanocarbons and the  $sp^2$  character of electrons in the basal planes. The defects allow the anchoring of carbonyl groups dehydrogenating ethylbenzene to styrene and therefore the formation of surface OH-groups. The gas-phase oxygen dissociated on the basal planes of the graphite layers by delocalized  $\pi$ -electrons, diffuse to the hydroxyl groups to oxidize the OH groups with water molecules released.<sup>[15]</sup>

CMK-3 carbon can be efficiently used for ODH of ethyl benzene to styrene. Besides the outstanding stability, it gives a high styrene yield among the tested nanocarbons under the same reaction condition. The XPS and IR spectra of the CMK-3 before and after reactions confirm that the reaction mechanism is the same as that when nanocarbons are used. The presence of oxygenated species is essential for a good catalytic activity. However, CMK-3 acts in the reaction quite differently from nanocarbons. While no coke formation was observed when carbon nanotubes were used for this reaction, CMK-3 plays a “support” role for active coke that is formed during the ODH of ethyl benzene, as it is revealed by the catalytic performance in Figure 2. This is also indicated by the BET surface area and nitrogen isotherms of the CMK-3 and confirmed by the electron micrograph shown in Figure 5. Once this active coke is formed on the CMK-3, the material is stable. The microstructure of the CMK-3 carbon is similar to activated carbon showing a disordered long-range ordering of carbon atoms. Both carbon materials are characteristic for the high-surface area. Activated carbon is also active in the ODH of ethylbenzene to styrene, but deactivates rapidly until nearly no activity is exhibited.<sup>[16,17]</sup> The CMK-3 used in the present work exhibits an unusual stability that can be related with its unique structure: the larger, but well-ordered porosity of mesoporous carbon is advantageous for mass transport and good thermal stability. The specific surface area of the used mesoporous carbon after the reaction is still as high as  $211\text{ m}^2\text{ g}^{-1}$ , while the specific surface area of activated carbon typically decreases from above  $1000\text{ m}^2\text{ g}^{-1}$  to below  $80\text{ m}^2\text{ g}^{-1}$  after 24 hours of reaction.<sup>[22a]</sup>

## Conclusion

In conclusion, we demonstrate that the CMK-3 carbon exhibits both high activity and selectivity in oxidative dehydrogenation of ethylbenzene to styrene, as well as good stability when compared with other conventional catalysts. Both the initial material and the active coke formed during the initial stage of the reaction play an important role in the catalytic performance. XPS and IR techniques reveal that the surface oxygen functional groups formed during the reaction are the active sites for the reaction. The ordered mesopores of the CMK-3 carbon should be beneficial for mass transport in catalytic reaction exhibiting long time stability in contrast to activated carbon.

## Experimental Section

### Catalyst Synthesis

The CMK-3 ordered mesoporous carbon was synthesized using mesoporous silica of SBA-15 as a hard template.<sup>[3]</sup> Typically, mesoporous silica was impregnated with sucrose solution in the presence of sulfuric acid and dried at 323 K and subsequently at 433 K. Then the impregnation/drying step was repeated once. The obtained sample was carbonized under nitrogen atmosphere at 1173 K for 4 h. Finally, the obtained silica/carbon composite was stirred in a hydrofluoric acid solution (35%) for 12 h, then filtrated and washed with distilled water, and dried at 393 K overnight.

### Characterization

The XRD pattern was obtained by a Siemens D5005 diffractometer using  $\text{Cu}_{K\alpha}$  radiation. The nitrogen adsorption at 77 K was measured using a Micromeritics ASAP 2010m system. The samples were degassed for 10 h at  $300^\circ\text{C}$  before the measurements. Scanning electron microscopy (SEM) and transmission electron microscopy (TEM) experiments were performed on Hitachi S-4000 and Philips CM 200 electron microscopes, respectively. An electron energy-loss spectrometer (EELS) equipped on the Philips CM200 is used for the measurement of energy-loss spectra of carbon inner-shell electrons. The XPS experiments were carried out in a modified LHS/SPECS EA200 MCD system equipped with facilities for XPS ( $\text{Mg}_{K\alpha}$  1253.6 eV, 168 W power) measurements. XPS spectra areas have been corrected considering that C 1s peaks have the same area in all the samples. The binding energy determined from the C 1s peak was referenced at 284.4 eV. Attenuated total reflectance infrared spectra (IR) were obtained on a Perkin–Elmer System 2000 FTIR spectrometer by using a KBr wafer. Surface analysis was performed on a VG RSCA LABMK II spectrometer equipped with  $\text{Al}_{K\alpha}$  radiation. Textural properties (specific surface area, pore size, and so forth) were determined by nitrogen physisorption at  $-196^\circ\text{C}$ .

### Catalytic Test

Oxidative dehydrogenation (ODH) of ethylbenzene to styrene reaction was carried out in a quartz tube reactor (4 mm i.d.  $\times$  320 mm) at temperatures between 350 and  $400^\circ\text{C}$ , holding 0.06 g of catalyst particles between two quartz wool plugs in the isothermal zone. Ethylbenzene was evaporated at  $38.5^\circ\text{C}$  in a flowing mixture of helium and oxygen, with an ethylbenzene concentration of 2.6 vol. % and an ethylbenzene/oxygen ratio of 5. The total flow was  $5\text{ mL min}^{-1}$  or  $10\text{ mL min}^{-1}$ . The inlet and outlet gas analysis was performed on an online gas chromatograph equipped with two columns for simultaneous analysis of aromatics and permanent gases: a 5% SP-1200/1.75% bentone 34 packed column for the hydrocarbons and a carboxen 1010 PLOT column for the permanent gases, coupled to FID and TCD detectors, respectively.

## Acknowledgements

The work in Berlin was partly funded by the European Union FP6 programme (CANAPE project), by the Max Planck Society in the frame of EnerChem project, and partly supported by the Deutsche Akademiker-Austauschdienst (DAAD and PPP). The work in Changchun was supported by State Basic Research Project, NSFC (20573044)

- [1] a) R. Ryoo, S. H. Joo, S. Jun, *J. Phys. Chem. B* **1999**, *103*, 7743; b) S. Jun, S. H. Joo, R. Ryoo, M. Kruk, M. Jaroniec, Z. Liu, T. Ohsuna, O. Terasaki, *J. Am. Chem. Soc.* **2000**, *122*, 10712; c) S. Han, T. Hyeon, *Chem. Commun.* **1999**, 1955; C. D. Liang, S. Dai, *J. Am. Chem. Soc.* **2006**, *128*, 5316; Y. Meng, D. Gu, F. Q. Zhang, Y. F. Shi, H. F. Yang, Z. Li, C. Z. Yu, B. Tu, D. Y. Zhao, *Angew. Chem.* **2005**, *117*, 7215; *Angew. Chem. Int. Ed.* **2005**, *44*, 7053.
- [2] J. Lee, S. Yoon, T. Hyeon, S. M. Oh, K. B. Kim, *Chem. Commun.* **1999**, 2177.
- [3] S. H. Joo, S. J. Choi, I. Oh, J. Kwak, Z. Liu, O. Terasaki, R. Ryoo, *Nature* **2001**, *412*, 169.
- [4] J.-S. Yu, S. Kang, S. B. Yoon, G. Chai, *J. Am. Chem. Soc.* **2002**, *124*, 9382.
- [5] A. Vinu, C. Streb, V. Murugesan, M. Hartmann, *J. Phys. Chem. B* **2003**, *107*, 8297.
- [6] H. Zhou, S. Zhu, M. Hibino, I. Honma, M. Ichihara, *Adv. Mater.* **2003**, *15*, 2107.
- [7] A.-H. Lu, W. Schmidt, A. Taguchi, B. Spliethoff, B. Tesche, F. Schüth, *Angew. Chem.* **2002**, *114*, 3639; *Angew. Chem. Int. Ed.* **2002**, *41*, 3489.
- [8] C. Vix-Guterl, E. Frackowiak, K. Jurewicz, M. Friebe, J. Parmentier, F. Béguin, *Carbon* **2005**, *43*, 1293.
- [9] J. Lee, S. Yoon, S. M. Oh, C.-H. Shin, T. Hyeon, *Adv. Mater.* **2000**, *12*, 359.
- [10] L. Wang, S. Lin, K. Lin, C. Yin, D. Liang, Y. Di, P. Fan, D. Jiang, F.-S. Xiao, *Microporous Mesoporous Mater.* **2005**, *5*, 136.
- [11] H. Yang, Q. Shi, X. Liu, S. Xie, D. Jiang, F. Zhang, C. Yu, B. Tu, D. Zhao, *Chem. Commun.* **2002**, 2842.
- [12] A. H. Lu, W. Schmidt, N. Matoussevitch, H. Bönemann, B. Spliethoff, B. Tesche, E. Bill, W. Kiefer, and F. Schüth, *Angew. Chem.* **2004**, *116*, 4403; *Angew. Chem. Int. Ed.* **2004**, *43*, 4303.
- [13] a) A. Corma, *Chem. Rev.* **1997**, *97*, 2373–2420; b) M. E. Davis, *Nature* **2002**, *417*, 813; c) F. Schüth, *Angew. Chem.* **2003**, *115*, 3730; *Angew. Chem. Int. Ed.* **2003**, *42*, 3604; d) J. Lee, S. Han, T. Hyeon, *J. Mater. Chem.* **2004**, *14*, 478; e) A.-H. Lu, F. Schüth, *Adv. Mater.* **2006**, *18*, 1793.
- [14] a) G. Mestl, N. I. Maksimova, N. Keller, V. V. Roddatis, R. Schlögl, *Angew. Chem.* **2001**, *113*, 2122; *Angew. Chem. Int. Ed.* **2001**, *40*, 2066; b) N. Keller, N. I. Maksimova, V. V. Roddatis, M. Schur, G. Mestl, Y. V. Butenko, V. L. Kuznetsov, R. Schlögl, *Angew. Chem.* **2002**, *114*, 1962; *Angew. Chem. Int. Ed.* **2002**, *41*, 1885.
- [15] a) D. S. Su, N. Maksimova, J. J. Delgado, N. Keller, G. Mestl, M. J. Ledoux, R. Schlögl, *Catal. Today* **2005**, *102–103*, 110; b) J. Zhang, D. S. Su, A. Zhang, D. Wang, R. Schlögl, C. Hebert, *Angew. Chem.* **2007**, *119*, 7460; *Angew. Chem. Int. Ed.* **2007**, *46*, 7319; c) J. Delgado, X. W. Chen, D. S. Su, R. Schlögl, *J. Nanosci. Nanotechnol.* **2007**, *7*, 3495; d) J. Delgado, D. S. Su, G. Rebmann, N. Keller, A. Gajovic, R. Schlögl, *J. Catal.* **2006**, *244*, 126.
- [16] R. Dziembaj, P. Kustrowski, T. Badstube, H. Papp, *Top. Catal.* **2000**, *11/12*, 317.
- [17] M. F. R. Pereira, J. J. M. Órfão, J. L. Figueiredo, *Appl. Catal. A* **2001**, *218*, 307.
- [18] H. Darmstadt, C. Roy, S. Kaliaguine, S. J. Choi, R. Ryoo, *Carbon* **2002**, *40*, 2673.
- [19] H. Darmstadt, C. Roy, S. Kaliaguine, *Carbon* **1994**, *32*, 1399.
- [20] C. S. K. Singamsetty, C. U. Pittman, G. L. Booth, Guo-Ren He, Jr.-S. D. Gardner, *Carbon* **1995**, *33*, 587.
- [21] Y. Xie, P. M. A. Sherwood, *Chem. Mater.* **1990**, *2*, 293.
- [22] a) M. F. R. Pereira, J. J. M. Órfão, J. L. Figueiredo, *Appl. Catal. A* **1999**, *184*, 153; b) L. E. Cadús, L. A. Arrua, O. F. Gorrioz, J. B. Rivarola, *Ind. Eng. Chem. Res.* **1988**, *27*, 2241; c) J. A. Maciá-Agulló, D. Cazorla-Amorós, A. Linares-Solano, U. Wild, D. S. Su, R. Schlögl, *Catal. Today* **2005**, *102–103*, 248.
- [23] H. R. Thomas, *J. Am. Chem. Soc.* **1979**, *101*, 323–329.

Received: November 9, 2008

Revised: February 5, 2009

Published online: May 21, 2009